

The interactome of the N-terminus of band 3 regulates red blood cell metabolism and storage quality



Ferrata Storti Foundation

Aaron Issaiyan,¹ Ariel Hay,² Monika Dzieciatkowska,¹ Domenico Roberti,³ Silverio Perrotta,³ Zsuzsanna Darula,⁴ Jasmina Redzic,¹ Micheal P. Busch,⁵ Grier P. Page,⁶ Stephen C. Rogers,⁷ Allan Doctor,⁷ Kirk C. Hansen,¹ Elan Z. Eisenmesser,¹ James C. Zimring² and Angelo D'Alessandro¹

¹Department of Biochemistry and Molecular Genetics, University of Colorado Denver – Anschutz Medical Campus, Aurora, CO, USA; ²University of Virginia, Charlottesville, VA, USA; ³Università della Campania "L. Vanvitelli", Naples, Italy; ⁴Laboratory of Proteomics Research, Biological Research Center, Szeged, Hungary; ⁵Vitalant Research Institute, San Francisco, CA, USA; ⁶RTI International, Pittsburgh, PA, USA and ⁷University of Maryland, Baltimore, MD, USA

Haematologica 2021
Volume 106(11):2971-2985

ABSTRACT

Band 3 (anion exchanger 1; AE1) is the most abundant membrane protein in red blood cells, which in turn are the most abundant cells in the human body. A compelling model posits that, at high oxygen saturation, the N-terminal cytosolic domain of AE1 binds to and inhibits glycolytic enzymes, thus diverting metabolic fluxes to the pentose phosphate pathway to generate reducing equivalents. Dysfunction of this mechanism occurs during red blood cell aging or storage under blood bank conditions, suggesting a role for AE1 in the regulation of the quality of stored blood and efficacy of transfusion, a life-saving intervention for millions of recipients worldwide. Here we leveraged two murine models carrying genetic ablations of AE1 to provide mechanistic evidence of the role of this protein in the regulation of erythrocyte metabolism and storage quality. Metabolic observations in mice recapitulated those in a human subject lacking expression of AE1₁₋₁₁ (band 3 Neapolis), while common polymorphisms in the region coding for AE1₁₋₅₆ correlate with increased susceptibility to osmotic hemolysis in healthy blood donors. Through thermal proteome profiling and crosslinking proteomics, we provide a map of the red blood cell interactome, with a focus on AE1₁₋₅₆ and validate recombinant AE1 interactions with glyceraldehyde 3-phosphate dehydrogenase. As a proof-of-principle and to provide further mechanistic evidence of the role of AE1 in the regulation of redox homeostasis of stored red blood cells, we show that incubation with a cell-penetrating AE1₁₋₅₆ peptide can rescue the metabolic defect in glutathione recycling and boost post-transfusion recovery of stored red blood cells from healthy human donors and genetically ablated mice.

Introduction

Band 3, also known as anion exchanger 1 (AE1) because of its role in the exchange of chloride for bicarbonate anions,¹ is one of the main targets of oxidant stress during red blood cell (RBC) aging *in vivo* and in the blood bank.^{2,3} AE1 also regulates RBC metabolism to allow adaptation to hypoxia and oxidant stress.⁴ The N-terminal cytosolic domain of AE1 serves as a docking site for deoxygenated hemoglobin, with significantly higher affinity than for oxygenated hemoglobin.^{5,6} Based on this background, it has been proposed that hemoglobin, in addition to its central role of carrying oxygen from the lungs to peripheral tissues, may serve as the “oxygen sensor” that directs AE1 to regulate metabolism appropriately. Indeed, studies had provided compelling, albeit indirect evidence that, when not encumbered by deoxy-hemoglobin, the N-terminus of AE1 can bind to and, in so doing, inhibit the glycolytic enzyme glyceraldehyde 3-phosphate dehydrogenase (GAPDH).⁷⁻¹¹ Notably, RBC host approximately 10⁶ copies of both AE1 and GAPDH.⁴ A wealth of indirect evidence supports

Correspondence:

ANGELO D'ALESSANDRO
angelo.dalessandro@ucdenver.edu

JAMES C ZIMRING
jc2k@virginia.edu

Received: December 24, 2020.

Accepted: February 26, 2021.

Pre-published: May 13, 2021.

<https://doi.org/10.3324/haematol.2020.278252>

© 2021 Ferrata Storti Foundation

Material published in *Haematologica* is covered by copyright. All rights are reserved to the Ferrata Storti Foundation. Use of published material is allowed under the following terms and conditions:
<https://creativecommons.org/licenses/by-nc/4.0/legalcode>. Copies of published material are allowed for personal or internal use. Sharing published material for non-commercial purposes is subject to the following conditions:
<https://creativecommons.org/licenses/by-nc/4.0/legalcode>, sect. 3. Reproducing and sharing published material for commercial purposes is not allowed without permission in writing from the publisher.



the likelihood and biological relevance of AE1-GAPDH interactions, based on data from immunofluorescence-based experiments,^{7,8} enzymatic activity assays, metabolic flux analysis via nuclear magnetic resonance (NMR),⁹ analytical ultracentrifugation,¹⁰ *in silico* prediction,¹¹ and genetic ablation of the N-terminus of band 3 in mice.¹² However, early crosslinking studies had hitherto failed to produce direct evidence of an interaction of GAPDH with the N-terminal residues.⁷ Nevertheless, a widely accepted model was proposed, according to which AE1 serves as a “railway switch” diverting glucose down different tracks (glycolysis vs. the pentose phosphate pathway [PPP]) depending on cellular needs.^{8,13,14} This model explains why, when oxidant stress is high and GAPDH is bound to AE1 and thereby inhibited, RBC favor glucose oxidation via the PPP, to generate the reducing cofactor NADPH and fuel related antioxidant systems;¹⁵ on the other hand, RBC would rely on glycolysis when oxidant stress is low (e.g., at high altitude¹⁶), hemoglobin is deoxygenated and binds to the N-terminus of AE1, which in turn favors the release of glycolytic enzymes from the membrane to promote the generation of energy in the form of ATP and NADH. Regulation of the balance between glycolysis and PPP is essential in order for RBC to be able to respond to their particular metabolic needs (membrane pump function, cytoskeleton and lipid homeostasis), which are a function of whether the RBC are exposed to high or low oxygen tensions in the lungs or peripheral capillaries.¹⁷

We and others have proposed that this balance may be dysregulated as RBC age and/or become damaged as a result of pathology (including SARS-CoV-2 infection¹⁸) or iatrogenic intervention (e.g., blood storage),^{19,20} depriving RBC of critical metabolic plasticity and leading to their demise.³ So far, the role of AE1 in the quality of stored RBC has only been hypothesized, based on a body of evidence that includes: (i) an increase in AE1 fragmentation as a function of oxidant stress in stored RBC;^{21–25} (ii) a progressive loss of the capacity to activate the PPP in stored RBC,^{26–28} despite the gradual inhibition of GAPDH as a function of its oxidation at the active site Cys152 and 156, His179;²⁹ (iii) an increase in band 3 phosphorylation at tyrosine (Y) residues as a function of storage,³⁰ which correlates with the release of microparticles from stored RBC; (iv) disruption of GAPDH localization in the membrane upon phosphorylation of Y8 and 21 of AE1;^{1,11,31} (v) a poorer storage quality and post-transfusion recovery of RBC from donors who are incapable of activating the PPP because of deficient glucose 6-phosphate dehydrogenase (G6PD) activity;^{32,33} and (vi) changes in AE1 oligomeric structure correlate with the loss of phospholipid asymmetry in stored RBC, which could affect survival upon transfusion.^{3,34} Despite this evidence, the role of AE1 in the quality of stored blood has not yet been elucidated mechanistically.

Methods

The methods are detailed extensively in the *Online Supplementary Methods*.

Animal studies with mice

All the animal studies described in this manuscript were reviewed and approved by the University of Virginia Institutional Animal Care and Use Committee (protocol n: 4269). Band 3 mouse founders, including huB3, HA Del and BS KO mice (see

later), originally generated by Chu *et al.*,³⁵ were acquired from the National Institutes of Health mouse embryo repository and were bred with C57BL/6 females. The use of Ubi-GFP and HOD mice has been described in prior publications by our group.³⁶ Whole blood was drawn by cardiac puncture as a terminal procedure for the mice.

Band 3 Neapolis

RBC (100 µL) were obtained from a subject carrying a mutation resulting in the lack of AE1 amino acids 1-11, as extensively described by Perrotta *et al.*³¹

REDS-III RBC Omics

Details of the Recipient Epidemiology and Donor assessment Study (REDS)-III RBC Omics, including the patients' enrollment, blood processing, osmotic hemolysis and development of the transfusion medicine genome-wide genotyping array have been described extensively in prior studies on the background of the project.^{33,37,38}

Methylene blue treatment, red blood cell storage and tracing experiments

RBC from wild-type (WT) and band 3 knockout (KO) mice were incubated with methylene blue (100 µM, Sigma Aldrich) at 37°C for 1 h, as described elsewhere.³²

RBC from the four main mouse strains investigated in this study, along with 13 different mouse strains described before,³⁹ were collected, processed, stored, and transfused and post-transfusion recovery was determined as previously described.³⁹

Tracing experiments were conducted with labeled glucose, citrate, glutamine, arachidonic acid and methionine. RBC (100 µL) from all the mouse strains investigated in this study or RBC lysates from healthy donor volunteers (n=8) or the individual carrying band 3 Neapolis RBC were incubated at 37°C for 1 h in the presence of stable isotope-labeled substrates, as described previously.²³

Metabolomics and proteomics

Metabolomics analyses were performed using a Vanquish ultra-high performance liquid chromatograph (UHPLC) coupled online to a Q Exactive mass spectrometer (Thermo Fisher, Bremen, Germany), as described previously.^{40,41}

Proteomics analyses, thermal proteome profiling and crosslinking experiments were performed via FASP digestion and nanoUHPLC tandem mass spectrometry identification (Thermo Fisher), as previously described.^{42,43} and extensively detailed in the *Online Supplementary Methods*.

Isothermal titration calorimetry

All isothermal titration calorimetry binding experiments were performed with a MicroCal iTC₂₀ (Cytiva) set at 25°C. GAPDH and band 3 proteins were dialyzed into matching buffer (20 mM Bis-Tris pH 6.5, 50 mM NaCl, 2 mM DTT). The cell contained GAPDH at 0.1 mM while the syringe contained band 3 at 1 mM. Reference power was set to 10 µcal/s with a constant stirring speed of 1,000 rpm. In total, 20 injections were performed. The first injection was excluded from the data analysis. Experiments were performed in duplicate and the results were analyzed with the Origin ITC module.

Nuclear magnetic resonance and structural models

¹⁵N-heteronuclear single quantum coherence (HSQC) spectra were collected at 25°C for the recombinantly expressed band 3 peptide 1-56 in the presence of 100 and 200 µM GAPDH. Data were collected on a Varian 900 using a standard ¹⁵N-HSQC sequence.

Results

Genetic ablation of the N-terminus of band 3 affects metabolism and glycolysis to pentose phosphate ratios in stored red blood cells

Despite similar function, the amino acid sequence of AE1 at the N-terminus is poorly conserved between mice and humans⁶ (Figure 1A). Low's group generated a knockin mouse by inserting the human binding site (amino acids 1-35) into the mouse AE1, resulting in a human-mouse hybrid AE1 (HuB3) that could be used for a reductionist analysis of the human binding motif.⁵ Two additional mouse models were subsequently made: (i) the first one carries a deletion of the first 11 amino acid residues - hereon referred to as high affinity deletion or HA Del, since deletion of these residues negatively affects binding of glycolytic enzymes, as suggested by immunofluorescence assays,^{7,8} enzymatic activity assays, metabolic flux analysis via NMR,⁹ analytical ultracentrifugation¹⁰, and *in silico* modeling;¹¹ (ii) the second model is characterized by a deletion of amino acid residues 12-23, which results in loss of affinity for the binding of deoxygenated hemoglobin (hereon referred to as binding site knockout or BS KO)³⁵ (Figure 1B). Based on this model (*Online Supplementary Figure S1A-C*), we hypothesized that blood from HA Del and BS KO mice would store poorly, because of the incapacity to activate the PPP as a result of the lack of residues 1-11 or 12-23, respectively, of the N-terminus of AE1 (Figure 1A, B). Importantly, genetic ablation of the AE1 N-terminus in these mice recapitulates the storage-induced fragmentation of the AE1 N-terminus at multiple residues in human RBC (*Online Supplementary Figure S1D*). RBC from WT, HuB3, HA Del and BS KO mice were stored under refrigerated conditions for 12 days, prior to metabolomics and unsupervised multivariate analyses (Figure 1C, D; *Online Supplementary Table S1*). The latter highlighted a significant impact of genotype on the end-of-storage levels of metabolites involved in glycolysis, the PPP and glutathione homeostasis (Figure 1E; *Online Supplementary Figure S2A, B*). To further investigate the impact on glycolysis and the PPP, RBC from these four mouse strains were incubated with 1,2,3-¹³C₃-glucose upon stimulation with methylene blue (MB) (Figure 1F). MB is metabolized into leukomethylene blue in a reaction that consumes NADPH and thus promotes PPP activation by law of mass action.³² The levels of lactate isotopologues 2,3-¹³C₂ and 1,2,3-¹³C₃ – and their ratios – are indicative of activation of the PPP and glycolysis, respectively, since the first carbon atom of 1,2,3-¹³C₃-glucose is lost in the form of ¹³CO₂ in the oxidative phase of the PPP (Figure G-I, *Online Supplementary Figure S2C*). Activation of the PPP following MB stimulation was comparable in WT, HuB3 and BS KO mouse RBC, but ablated in HA Del mice; the defect in PPP activation of HA Del mice was rescued, while BS KO mouse RBC had higher basal levels and further increases in PPP activation by MB when incubated with the AE1₁₋₃₅ peptide (Figure 1I; *Online Supplementary Figure S2C*).

Red blood cells from mice lacking the N-terminus of band 3 have poorer post-transfusion recovery

Fresh and stored RBC from HA Del or BS KO mice also showed increased levels of carboxylic acids (succinate, fumarate, malate), acyl-carnitines (hexanoyl-, decanoyl-, dodecenoyl-, tetradecenoyl- and hexadecanoyl-carnitine) and lipid peroxidation products compared to WT and HuB3 mouse RBC, especially with regard to metabolites of the

arachidonic and linoleic acid pathways (Figure 2A-C). Tracing experiments with labeled glutamine, citrate and methionine confirmed the steady-state aberrations in AE1 KO mice following MB challenge, while incubation with a recombinant AE1₁₋₃₅ peptide only rescued glutaminolysis in HA Del mice and malate generation in BS KO mice (Figure 2A-C).

Expanding on previous targeted metabolomics studies,^{36,39} untargeted metabolomics analyses on fresh and stored RBC from 13 different mouse strains identified metabolic correlates of post-transfusion recovery (Figure 2D-G), a Food and Drug Administration gold standard for storage quality. Pathway analyses and top ranked correlates are shown in Figure 2E-G, including previously reported oxylipins,^{36,39} but also purine oxidation products (xanthine), short chain and long chain saturated fatty acids, as well as carboxylic acids as top negative correlates (Figure 2F, G; *Online Supplementary Table S1*). All of these metabolites accumulated at higher levels in stored RBC from HA Del and BS KO mice compared to WT and HuB3 mice. Consistently, determination of end-of-storage post-transfusion recovery of RBC from the four mouse strains showed significant decreases in post-transfusion recovery in the HA Del and BS KO mice (63.2±3.1% and 35.4±5.8%, respectively compared to 88.9±5.6% for WT and 85.5±3.6% for HuB3 mouse RBC) (Figure 2H).

Lack of the 11 N-terminal amino acids of AE1 in humans results in red blood cell metabolic alterations comparable to those in AE1 knockout mice

In 2005, Perrotta and colleagues³¹ identified a son of a consanguineous marriage with severe anemia, which was associated with a deficiency of AE1 expression (~10% of normal levels). Characterization of the gene coding for AE1 (*SLC4A1*) revealed a single base substitution (T-->C) at position +2 in the donor splice site of intron 2, resulting in the generation of a novel mutant protein that lacked residues 1-11 (band 3 Neapolis) (Figure 3A). The HA Del mice in this study recapitulate, at least in part, band 3 Neapolis RBC in humans. Consistent with observations in HA Del mice, “omics” analyses of band 3 Neapolis RBC compared to control RBC showed significant alterations of glycolysis, glutathione homeostasis, decreases in methyl-group donors for isoaspartyl damage repair,²³ increases in carboxylic acid, and altered arginine and polyamine metabolism (Figure 3B; *Online Supplementary Figure S3A, B*). Incubation of band 3 Neapolis RBC lysates with 1,2,3-¹³C₃-glucose confirmed a deficit in the capacity to activate the PPP following stimulation with MB, a defect that was corrected by rescue with a recombinant AE1₁₋₃₅ peptide (Figure 2C), similar to HA Del RBC.

Proteomics analyses showed higher levels of hexokinase, but lower levels of all the remaining glycolytic enzymes downstream to it, as well as of enzymes of the PPP and glutathione synthesis in the RBC from the band 3 Neapolis individual (*Online Supplementary Figure S4C*), despite comparable mean corpuscular value, mean corpuscular hemoglobin and hematocrit (*Online Supplementary Table S1*). Alterations in RBC metabolism in band 3 Neapolis RBC comparable to those observed in AE1 KO mice were confirmed not just at steady state (e.g., higher levels of lipid oxidation products) (Figure 3D), but also by tracing experiments with ¹³C¹⁵N-glutamine; ¹³C-citrate, ¹³C¹⁵N-methionine, and deuterium-labeled arachidonate (*Online Supplementary Figure S3D-G*).

Single nucleotide polymorphisms in the region coding for AE1_{iso} correlate with increased osmotic fragility of stored human red blood cells

Mutations targeting the N-terminus of AE1 (e.g., AE1_{iso}, band 3 Neapolis) in humans result in significant hemolysis, requiring blood transfusion.³¹ Therefore, humans carrying equivalent mutations to those used in our mechanistic mouse models would not be eligible to donate blood. The region coding for AE1 (gene name *SLC4A1*) is highly polymorphic in humans. AE1 polymorphisms were captured in the genetic array of over 879,000 single nucleotide polymorphisms designed for the Recipient Epidemiology

and Donor assessment Study (REDS) III-RBC Omics.³⁷ The REDS III RBC Omics enrolled a large cohort of 13,806 healthy donor volunteers in four different blood centers across the USA.³³ Units from these donors were stored for up to 42 days prior to determination of the RBC susceptibility to hemolysis following osmotic insults.³⁸ Genome-wide association studies revealed that the highly polymorphic region on chromosome 17 coding for AE1 ranked among the top correlates with osmotic fragility (Figure 3E). While the most significant single nucleotide polymorphisms associated with greater osmotic hemolysis were intronic variants, three polymorphisms were identified in

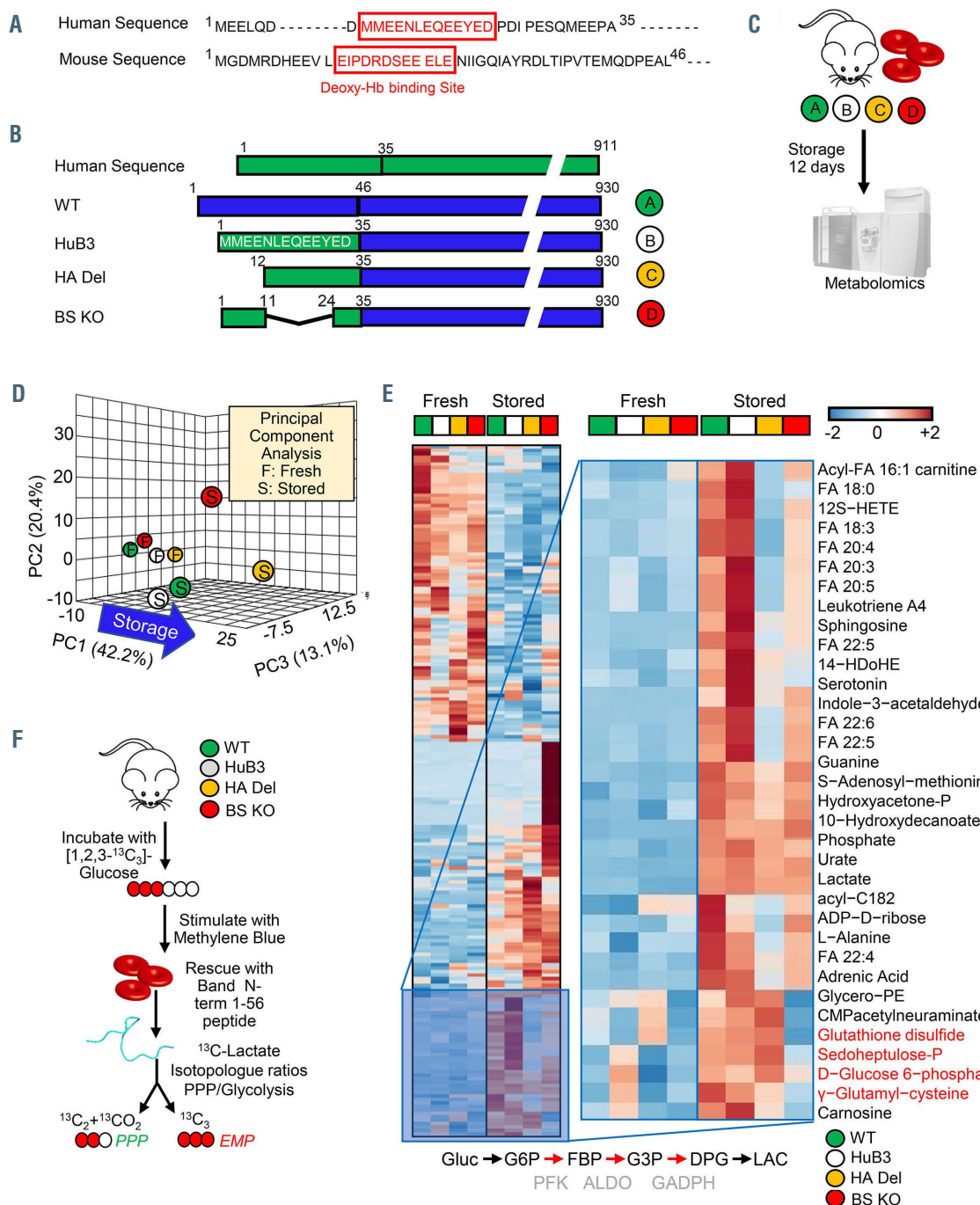


Figure 1. Continued on the following page.

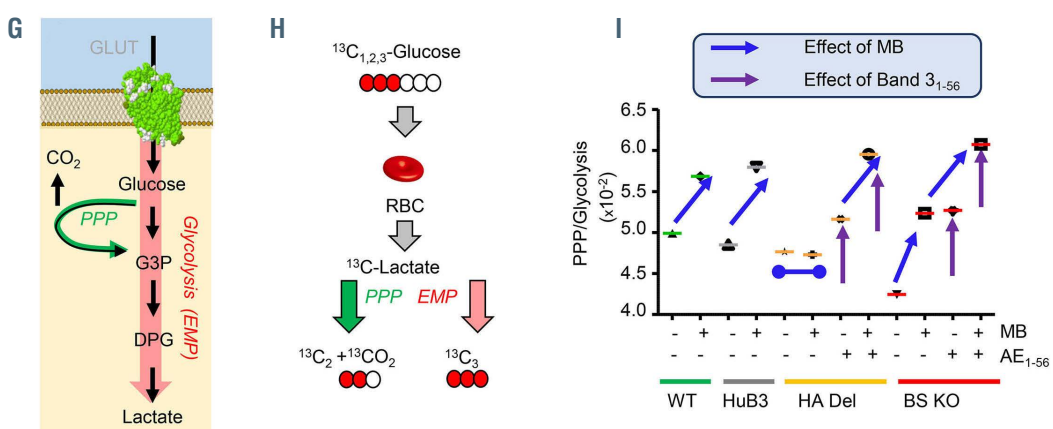


Figure 1. The N-terminus of band 3 controls red blood cell metabolism during storage under blood bank conditions. (A) Human and mouse N-terminal band 3 sequences are slightly different. (B) We leveraged humanized AE1 mice,¹² and compared them to wild-type (WT) mice (C57BL6), or humanized mice lacking residues 1-11 (deletion of the high affinity binding region for glycolytic enzyme;¹² HA Del) or 12-23 (hemoglobin binding site knockout; BS KO). (C) Red blood cells (RBC) from these mice were stored under refrigerated conditions for 12 days, prior to metabolomics analyses. (D) Storage and genotypes had a significant impact on RBC metabolism, as determined by unsupervised principal component analysis (D) and hierarchical clustering analysis of significant metabolites by analysis of variance (E). Specifically, strain-specific differences in fresh and stored RBC were noted in glycolysis, the pentose phosphate pathway (PPP) and glutathione homeostasis. (F) To further investigate the impact on glycolysis and the PPP, RBC from the four mouse strains were incubated with 1,2,3-¹³C-glucose upon stimulation with methylene blue (MB). (G, H) Rescue experiments were also performed by incubating RBC with a recombinantly expressed N-terminus AE1 peptide (residues 1-56), prior to determination of the ratios of lactate isotopologues +3 and +2, deriving from glycolysis and the PPP, respectively. (I) MB activated the PPP in all mouse strains except for the HA Del mice. Supplementation of the AE1₁₋₅₆ peptide increased PPP activation and decreased glycolysis in HA Del mice and further exacerbated responses in all the other strains.[±]

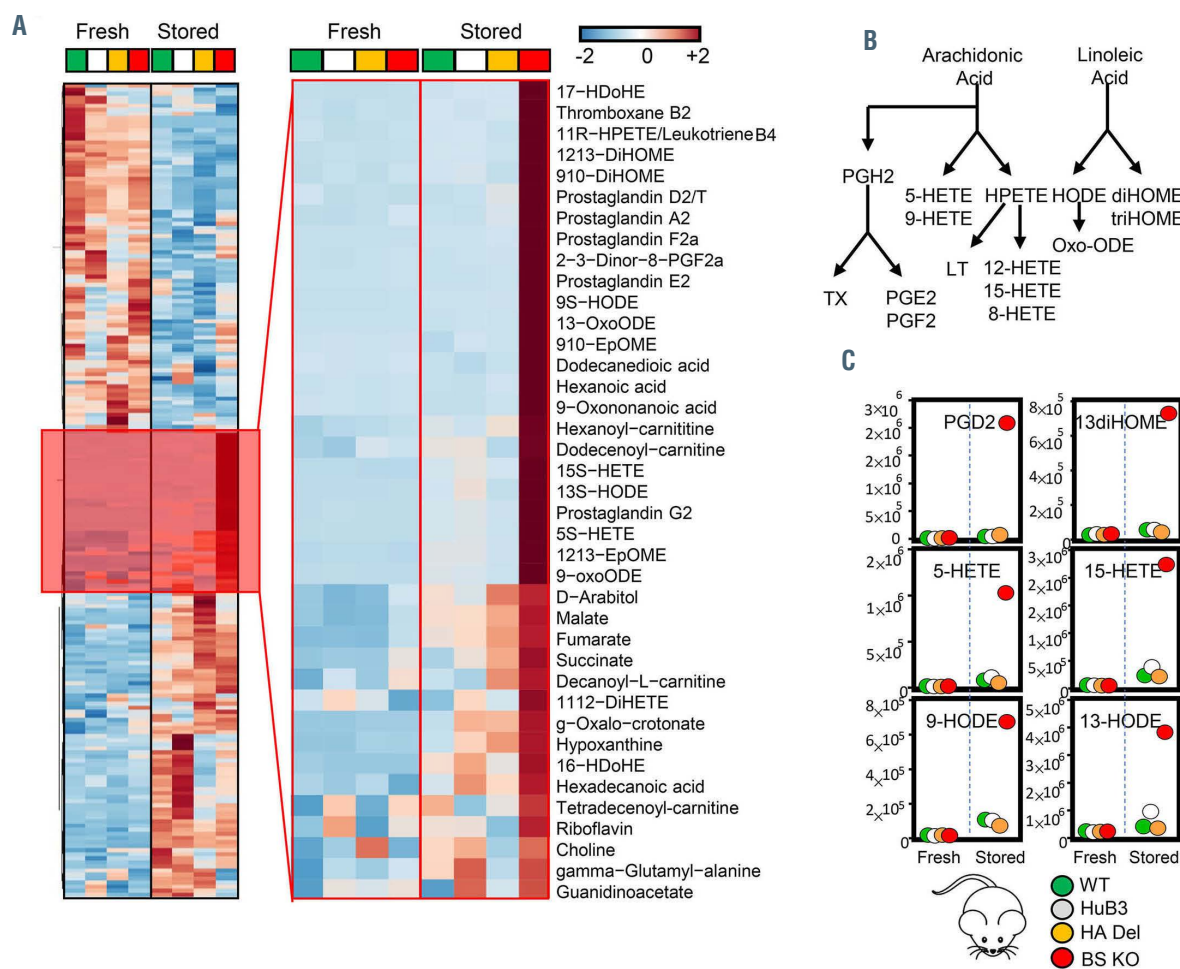


Figure 2. Continued on the following page.

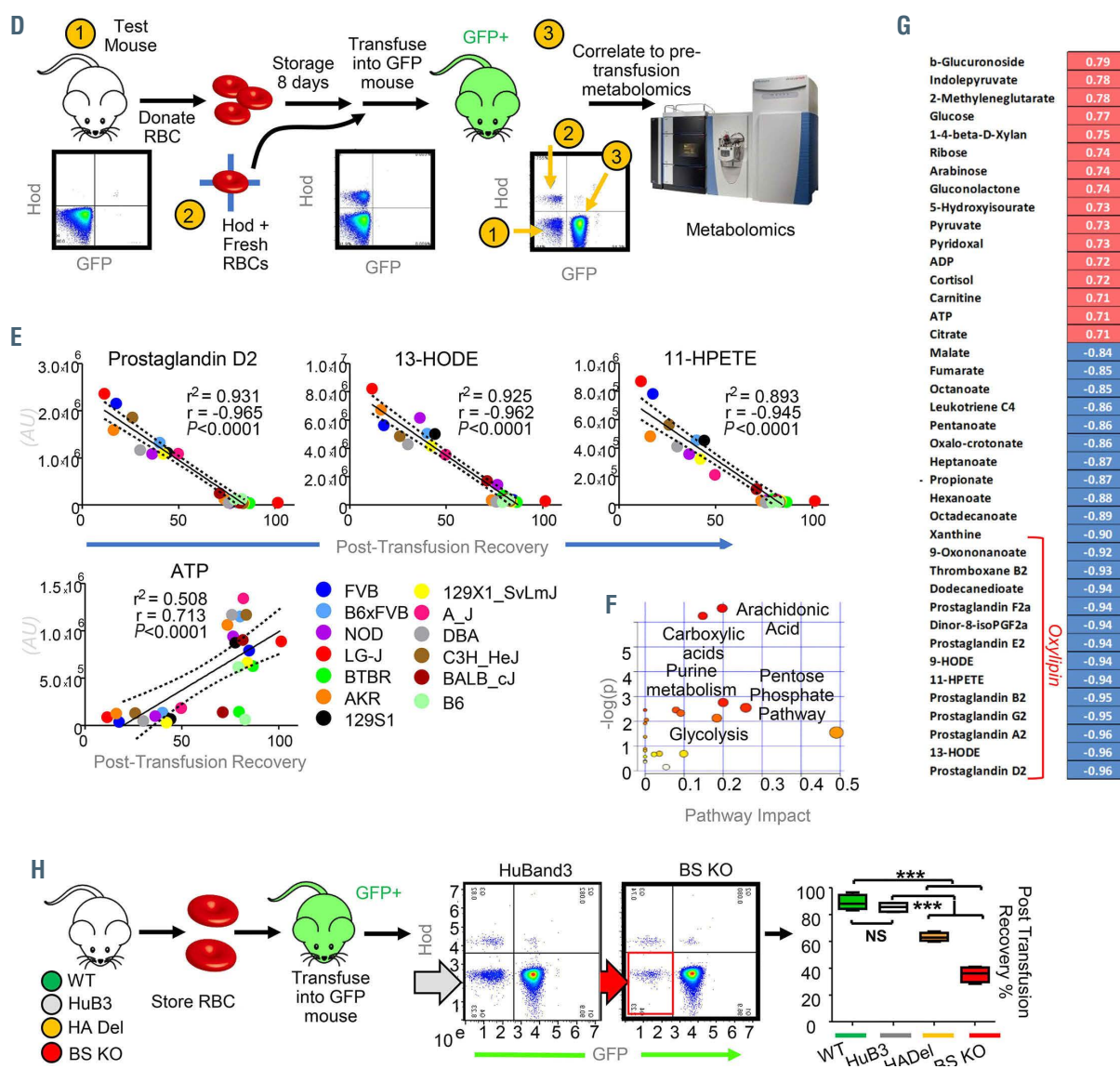


Figure 2. Metabolic alterations in band 3 knockout mice correlate with poor post-transfusion recovery. (A-C) Analyses of fresh and stored red blood cells (RBC) from wild-type (WT) (C57BL6) mice [green], humanized band 3 mice (HuB3) [white] and mice lacking amino acids 1-11 (HA Del) [yellow] or 12-23 (BS KO) [orange] of band 3 showed strain-specific differences in several pathways in fresh and stored RBC. Above all, stored RBC from the KO mice were characterized by increased levels of carboxylic acid and lipid peroxidation products (A), especially metabolites of the arachidonate metabolism (B), including prostaglandins, eicosanoids, hydroxyeicosatetraenoates (HETE) and hydroxyoctadecenoates (HODE) (C); the full, vectorial version of this list is provided in *Online Supplementary Table S1*. (D-F) Metabolomics analyses on fresh and stored RBC from 13 different mouse strains (D) highlight these metabolites as significant correlates with poor post-transfusion recovery (E), as highlighted by the metabolite set enrichment analysis in (F) and the ranked top positive and negative correlates with post-transfusion recovery reported in (G). (H) Determination of end-of-storage post-transfusion recovery of RBC from the four mouse strains showed significant decreases in recovery in the HA Del and BS KO mice.

the blood donor population as D38A, E40K and K56E. These single nucleotide polymorphisms had been previously reported to be associated with hereditary spherocytosis (band 3 Foggia and Neapolis II),^{44,45} a condition associated with mild to moderate hemolysis in eligible blood donors,⁴⁶ especially when heterozygous for these traits. The D38A allele was rare in Europeans (4% of the donor population) and relatively more common in east Asians (8%), while the K56E allele was common in donors of African ancestry (10%). Although low, these allele frequencies appear to be relevant to the field of transfusion medicine when considering the over 100 million units donated every year around the world.

Proteomics and structural studies on the interactome of band 3

After confirming the lack of the N-terminal portion of AE1 in the KO mice (*Online Supplementary Figure S4E-G*), we characterized the proteomes of RBC from the four mouse strains, with a focus on protein levels that were similarly altered in both HA Del and BS KO mice, or uniquely altered in either KO strain (*Online Supplementary Figure S4H-K*). The list of proteins whose levels were decreased in band 3 KO mice included numerous proposed interactors of AE1 (in red in *Online Supplementary Figure 4H-K*, *Online Supplementary Table S1*). This observation could be explained by altered protein expression in erythroid cells

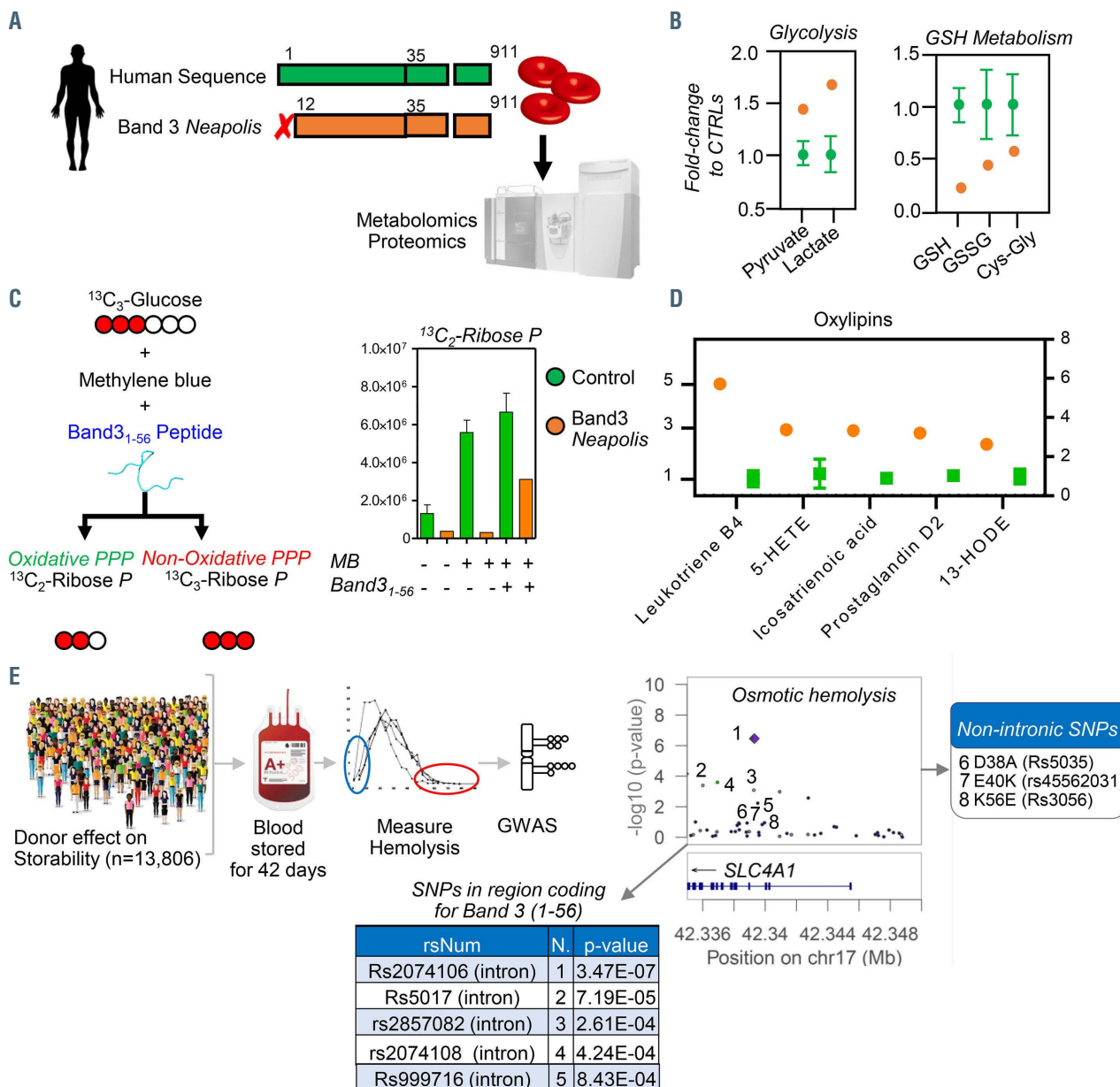


Figure 3. Metabolic impact of AE1₁₋₅₆ deletion in human red blood cells and alterations of osmotic fragility of stored red blood cells from donors with polymorphisms in AE1₁₋₅₆. (A, B) Lack of amino acid residues 1-11 of AE1 in humans, known as band 3 Neapolis, (A) results in increased activation of glycolysis and decreases in glutathione pools (B). (C) Tracing experiments with 1,2,3-¹³C-glucose showed impaired responses to methylene blue (MB)-induced activation of the pentose phosphate pathway (PPP) compared to glycolysis in band 3 Neapolis, a phenotype that is partially rescued *in vitro* by supplementation of a recombinant AE1₁₋₅₆ peptide. (D) However, band 3 Neapolis RBC were also characterized by higher levels of oxylipins, comparable to those observed in stored RBC from mice lacking AE1 amino acids 12-23 (BS KO). (E) Genome-wide association studies on 13,806 healthy donor volunteers revealed increased osmotic fragility in subjects carrying a polymorphism in the region coding for band 3 (gene name SLC4A1) residues 1-56 and neighboring introns. CTRL: control; GSH: reduced glutathione; GSSG: oxidized glutathione; HETE: hydroxyeicosatetraenoates; HODE: hydroxyoctadecenoates; GWAS: genome-wide association studies, SNP: single nucleotide polymorphisms.

during maturation to RBC, or could be indicative of a protective role from proteolytic degradation by interaction of these proteins with the N-terminus of AE1, as proposed in other studies of the RBC degradome.⁴⁷

To test the latter hypothesis, we used thermal proteome profiling coupled to tandem mass tag 10 (TMT10) (Figure 4A) to determine candidate interacting partners to AE1₁₋₅₆. Candidate interactors were identified as those with the most extreme alterations in the temperature at which their solubility decreased/increased and precipitation was observed (ΔT_m) (Figure 4B, *Online Supplementary Table S1*). In other words, an increase/decrease in the ΔT_m of a pro-

tein indicates a stabilizing/destabilizing effect on the protein (or the complex it is part of) through direct/indirect interaction with AE1₁₋₅₆. A few representative melting curves for the top hits for proteins stabilized or destabilized by the presence of AE1₁₋₅₆ (red) compared to untreated controls (blue) are provided in Figure 4C. Hits include several glycolytic enzymes GAPDH, aldolase A, phosphoglycerate kinase and lactate dehydrogenase A; hemoglobin α and beta; enzymes involved in redox homeostasis and oxidant damage-repair such as protein L-isospartate O-methyltransferase, peroxiredoxin 2, γ -glutamyl cysteine ligase, glyoxalase 1, aldehyde dehydrogenase 1, glutathione peroxy-

dase 4, and phosphogluconate dehydrogenase; or other metabolic enzymes including acetyl-CoA lyase, arginase 1, adenosyl homocysteine hydrolase, glutamate oxalacacetate transaminase, and adenylate kinase (Figure 4C).

Immunoprecipitation and crosslinking proteomics studies with recombinantly expressed AE1₁₋₅₆

To confirm and expand on the thermal proteome profiling-TMT10 analyses, we recombinantly expressed AE1₁₋₅₆ with a His-SUMO-tag at either the N- or C-terminus, prior to incubation with human plasma, RBC cytosols and membrane from human RBC lysates and purification/pull-down of interacting partners (*Online Supplementary Figure S5A*). Pathway analyses of the hits from these experiments confirmed most of the hits from thermal proteome profiling (*Online Supplementary Table S1*), revealing a widespread network of interactors of AE1, including up to 63 proteins involved in metabolic regulation, as mapped against the KEGG pathway map of human metabolism (*Online Suppl*

Supplementary Figure S5B, C). One limitation of the thermal proteome profiling and immunoprecipitation approaches is that they identify both direct and indirect interactors to AE1 that can be pulled down because of their complexing with direct AE1 interactors. To distinguish between direct and indirect interactors of AE1₁₋₅₆, we repeated the precipitation experiments by also introducing crosslinking agents, disuccinimidyl sulfoxide (DSSO) or 4-(4,6-dimethoxy-1,3,5-triazin-2-yl)-4-methylmorpholinium (DMTMM) (*Online Supplementary Figure S6A, B; Online Supplementary Table S1*). As proof of principle, we first performed these analyses on RBC lysates without the addition of recombinant AE1, providing an experimental report of the RBC interactome (shown in the form of a circos plot or network view in *Online Supplementary Figure S6C, D*, respectively; *Online Supplementary Table S1*), significantly expanding on *in silico* predictions reported in the literature.⁴⁸ This analysis recapitulated decades of structural studies on RBC hemoglobin (*Online Supplementary Figure S7*) and the RBC membrane

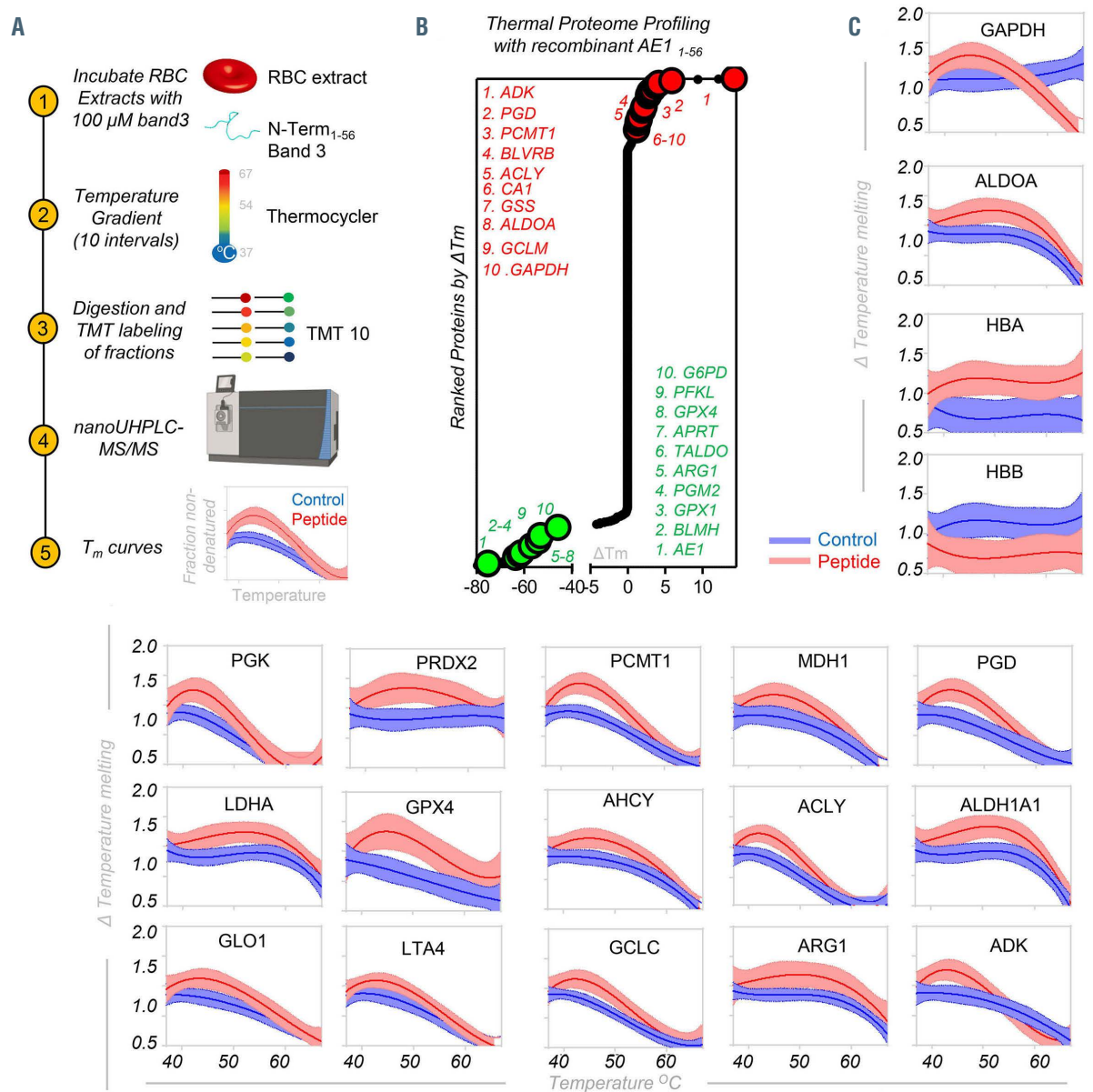


Figure 4. Continued on the following page.

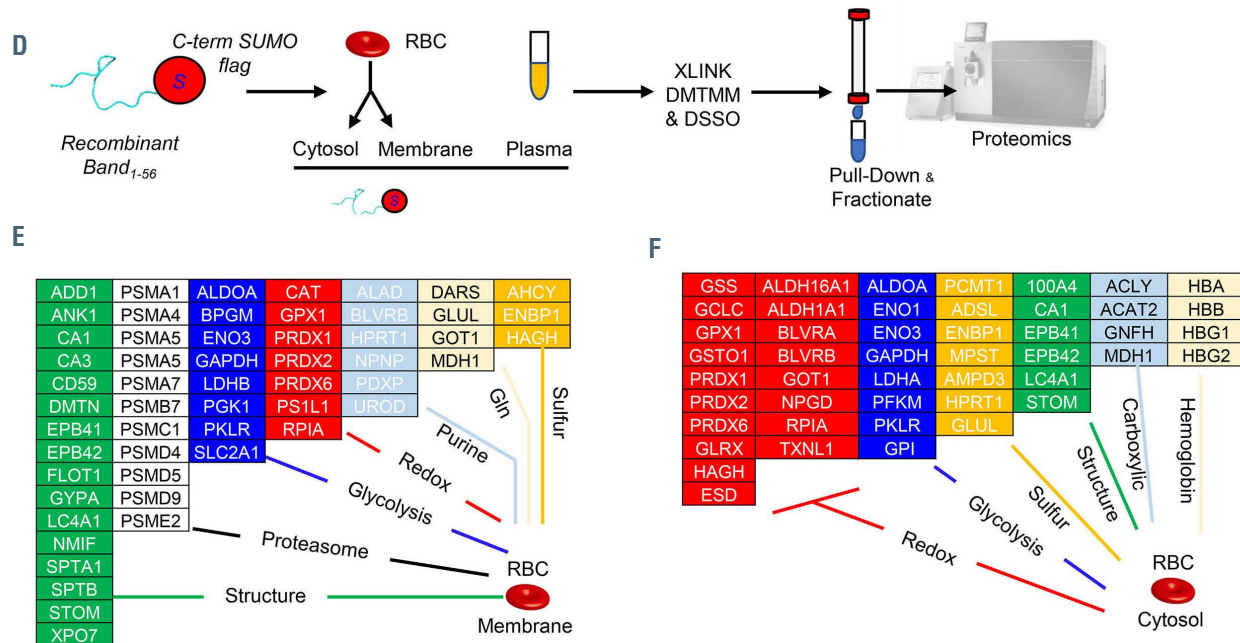


Figure 4. Thermal proteome profiling and crosslinking proteomics of recombinant peptide 1-56 of band 3 in red blood cell lysates. (A) Thermal proteome profiling experiments were performed by incubating red blood cell (RBC) lysates with a recombinantly expressed peptide coding for the amino acids 1-56 in the N-terminus of band 3 at a gradient of temperatures from 37 °C to 67 °C, labeling with ten different tandem mass tags (TM10), pooling and analysis via nano-ultrahigh performance liquid chromatography tandem mass spectrometry (nanoUHPLC-MS/MS). (B) Proteins were ranked as a function of their alterations in the temperature at which their solubility decreases and precipitation is observed (ΔT_m). (C) A few representative melting curves for the top hits for proteins stabilized or destabilized by the presence of the band 3 peptide 1-56 (red) compared to untreated controls (blue) are provided. (D) A peptide coding for amino acids 1-56 of the N-terminus of band 3 was recombinantly expressed with a SUMO-tag and/or a His-Flag tag at either the N- or C-terminus of the peptide, prior to incubation with plasma, RBC cytosols and membrane in independent experiments, enrichment in nickel columns, pull-down against the SUMO tag, and crosslinking (XLINK) with disuccinimidyl sulfoxide (DSSO) or 4-(4,6-dimetoxy-1,3,5-triazin-2-yl)-4-methylmorpholinium (DMTMM), prior to protein digestion, fractionation of crosslinked peptides and nanoUHPLC-MS/MS-based identification of band 3 interacting partners via MS2/MS3 analyses. (E, F) Top interactors for RBC membrane and cytosol interactors are listed in (E) and (F), respectively, divided by pathway.

interactome (*Online Supplementary Figure S8A-C*), relevant to the regulation of the RBC cytoskeleton, and the role AE1 plays as a lynchpin for RBC membrane structural proteins (*Online Supplementary Figure S8C*) and AE1 multimerization in the intra- and extra-cellular compartments (*Online Supplementary Figure S8D, E*). A detailed description and discussion of these results is provided in the *Online Supplementary File*.

To further focus on the AE1 N-terminus, crosslinking proteomics studies were repeated with the addition of recombinant AE1₁₋₅₆. This approach enabled determination of direct AE1₁₋₅₆ protein interactors by identifying crosslinked free ε-amines of lysine (K) with adjacent identical residues (DSSO) or carbon atoms in the carboxylic groups of aspartic acid (D) or glutamic acid (E) (DMTMM) (Figure 5), provided these residues face each other within a range spanning from 11.4 to 24 Å.⁴⁹ The list (*Online Supplementary Table S1*) included several structural proteins, proteasomal components, and enzymes involved in glycolysis, redox homeostasis, and purine, glutamine or sulfur metabolism, both in RBC membranes and cytosols (Figure 4E, F, respectively). An overview of the AE1₁₋₅₆ interactome is shown in Figure 5. This approach revealed three hot spots of crosslinks, at D or E residues in amino acid sequences 1-7, 13-25 and 40-45 of the AE1 N-terminus (Figure 5). Intramolecular and intermolecular interactions were observed for AE1 itself at the N-terminus (positions 45-6; 45-38; 45-56; 45-1; 25-1, 38-1, etc.) and C-terminus (833-840; 837-765; 771-849, etc.) (*Online Supplementary Table S1*). We report direct interactions of AE1₁₋₅₆ with hemoglobin B (1-2; 25-2; 23-2; 10-2; 10-134; 1-97; 38-2; 6-2; 1-100) (*Online Supplementary Figure S9*) and

hemoglobin A (38-7, 38-86; 1-97: less frequently and with lower scores than the crosslinks with hemoglobin B).⁵ In addition, direct crosslinks were identified for AE1₁₋₅₆ with spectrin β (residues 23 to 1664), ankyrin (residues 10-381) (*Online Supplementary Figure S8A-C*), phosphoglucomutase 2 (residues 23-88), enolase β (residues 38-198), glyoxylase 2 (residues 10-299), Rab GDP dissociation inhibitor β (position 2-2) (*Online Supplementary Table S1*), Golgi integral membrane protein 4 (residues 23-570 – consistent with work on endosomes),⁵⁰ carbonic anhydrase 2 (residues 1-81) and biliverdin reductase B (residues 1-40).

Pull-down of AE1₁₋₅₆ followed by crosslinking studies identified further candidate indirect interactors that are part of macromolecular complexes with direct AE1₁₋₅₆ interactors, including peroxiredoxin 2,⁵¹ peroxiredoxin 6, catalase, phosphofructokinase isoforms,¹² proteins 4.1 and 4.2, glucose phosphate isomerase, stomatin, adducin β, carbonic anhydrase 1, and 1-phosphatidylinositol 4,5-bisphosphate phosphodiesterase η-2 (full list in *Online Supplementary Table S1*). Other enzymes were pulled-down, but not directly crosslinked (suggestive of an indirect interaction with AE1, although direct interactions with other residues beyond residue 56 cannot be ruled out), such as acetyl-CoA lyase, bleomycin hydrolase, serine/threonine-protein kinase OSR1, desmoplakin, calpastatin, and glycophorin A.

Biophysical studies of the GAPDH and AE1₁₋₅₆ interaction

The interaction between recombinant GAPDH tetramers (Figure 6A) and AE1₁₋₅₆ (also including K56) was confirmed via isothermal titration calorimetry with a Kd of 2.56 μM

(Figure 6B), and two-dimensional NMR upon titration of GAPDH (0, 100 and 200 μ M) (Figure 6C). Of note, recombinant expression of an AE1 peptide spanning from residues 1-30 resulted in weaker interactions with GAPDH (K_d : 44.8 μ M) (Online Supplementary Figure S10A, B). Calculations of chemical shift perturbations induced by GAPDH titration to the ^{15}N -labeled AE1₁₋₅₆ (Figure 6D) provided clues on the structural organization of the otherwise intrinsically disordered N-terminus of AE1. Specifically, residues that comprise the AE1 binding site exhibit severe line-broadening due to exchange with the much larger GAPDH. For example, the terminal residues are the primary binding site as illustrated by the near complete disappearance of the central Y8 amide, compared to the Y46 amide, which exhibits no chemical shift perturbations (Figure 6E). DSSO and DMTMM crosslinks of GAPDH and AE1₁₋₅₆ (a representative spectrum between AE1 K56 and GAPDH D203 is shown in Figure 6F) are reported in Figure 6G and Online Supplementary Table S1. Cross-linked residues are mapped against the GAPDH monomeric structure in Figure 6H. Similar results were obtained when probing interactions between GAPDH and AE1₁₋₅₆ (Online Supplementary Figure S10C-E), with the exception of crosslinks between E40, a hotspot for interaction with several GAPDH residues in the longer AE1 peptide (3, 5, 84, 86, 194, 219, 251, 259, 260, 263) (Figure 6G). These experiments provide further proof of a direct interaction of the N-terminus of AE1 with GAPDH and indicate that the N-terminal region comprising residues 1-20 is the primary binding site with additional contacts that also contribute to the AE1/GAPDH interaction. Isothermal titration calorimetry,

NMR and crosslinking proteomics data were used to build a model of the AE1₁₋₅₆ interaction with GAPDH with the Rosetta software, indicating that the active site pocket of GAPDH is exposed to residues 1-15 of AE1 (Figure 6I, K; distances between K and D/E residues are shown in Online Supplementary Figure S10F).

Cell membrane-permeable AE₁₋₅₆ peptides reverse the defect in glutathione recycling capacity of red blood cells from band 3 knockout mice

To rescue the genetic defect resulting from ablation of the AE1 N-terminus, we designed three membrane permeable versions⁵² of AE1₁₋₅₆ through addition of a polyarginine (polyArg), internalization sequence or TAT sequence at the C-terminus of the peptide (Figure 7A). Human RBC were thus incubated with a control (scramble), an AE1₁₋₅₆ peptide (non-penetrating) or the three cell-penetrating peptides in the presence of 1,2,3- $^{13}\text{C}_3$ -glucose and MB stimulation to activate the PPP (Figure 7A). Tracing experiments showed that the PPP was activated following MB in all cases, but ATP synthesis was only preserved in the RBC treated with the cell-penetrating peptides (Figure 7B), consistent with the schematic in Figure 7C. We thus hypothesized that incubation with polyArg-AE1₁₋₅₆ would at least partially rescue the defect in PPP activation upon MB stimulation of RBC from AE1 KO mice, especially HA Del (Figure 7D). The results showed increased glutathione oxidation (GSSG/GSH ratios) in response to MB treatment in all cases, but a significant rescue by the AE1 peptide in both AE1 KO. In the presence of polyArg-AE1₁₋₅₆ post transfusion recovery of stored murine RBC was restored in WT and HA

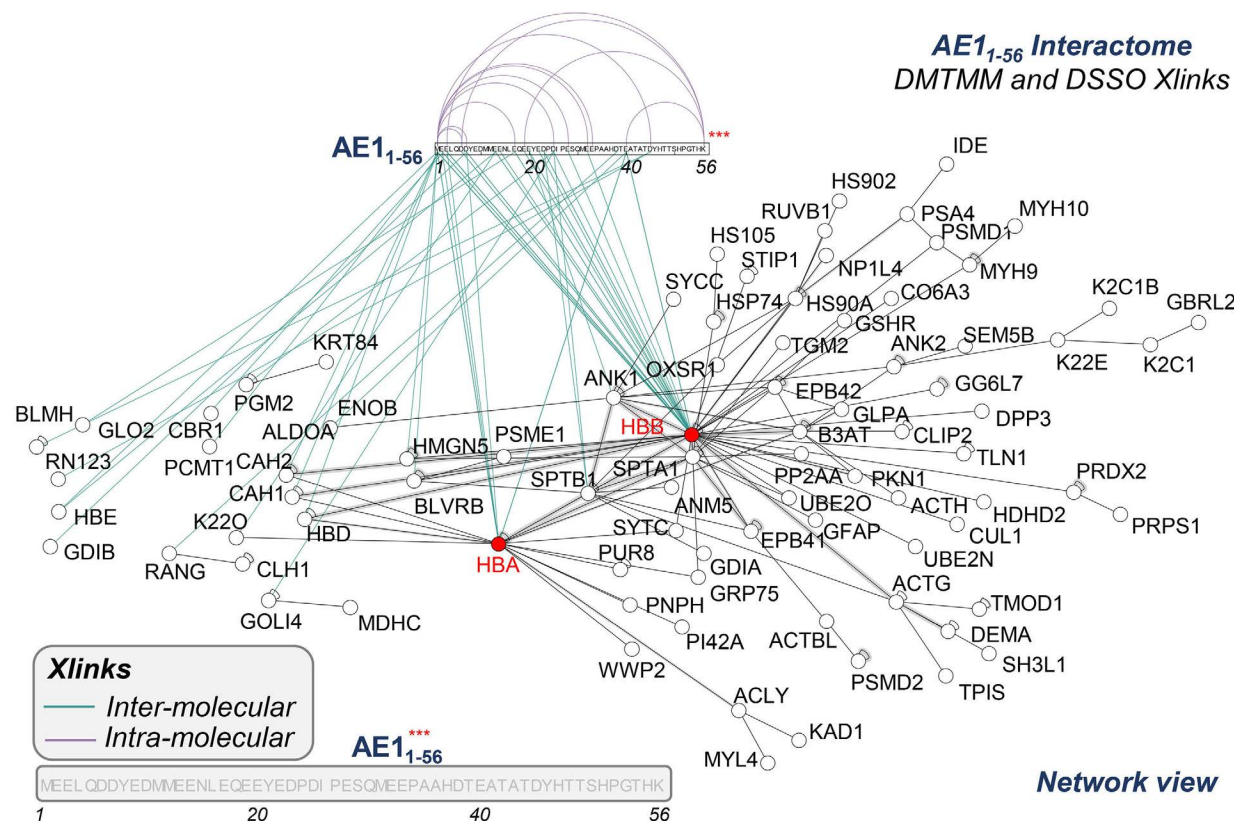


Figure 5. The interactome of AE1₁₋₅₆, as gleaned from crosslinking mass spectrometry. A network view of the interactome of AE1₁₋₅₆, as determined by merging the data from all the crosslinking proteomics studies. The network shows direct and indirect interactors with AE1₁₋₅₆ and the residues on band 3 with which the proteins were identified to crosslink (XLINK).

Del mice back to levels observed in HuB3, but not in BS KO mice (Figure 7E)

Discussion

Here we provide mechanistic evidence of a role for the N-terminus of AE1 in regulating the quality of stored RBC. Using multiple state-of-the-art direct and indirect structural approaches, we provide an experimental overview of the RBC interactome, with a focus on the N-terminus of band 3. A further discussion of the results is provided in the *Online Supplementary File*. While the structure of the N-terminus of AE1 beyond residue K56 has been solved through crystallography,⁵³ AE1₁₋₅₆ is an intrinsically disordered domain that has hitherto eluded structural studies. In the present study, we provide conclusive, direct evidence of the interaction between GAPDH and band 3 by: (i) thermal proteome profiling; (ii) pull-down and (iii) crosslinking of recombinantly expressed AE1₁₋₅₆; (iv) isothermal titration

calorimetry, (v) NMR, (vi) crosslinking with two different agents (DSSO and DMTMM) of recombinantly expressed GAPDH and AE1₁₋₅₆ or AE1₁₋₂₀ - the former showing a stronger interaction at least in part explained by a hotspot of crosslinks between E40 on AE1 and GAPDH. Of note, crosslinking studies have hitherto failed to show direct proximity of the (many) acidic residues of the AE1 N-terminus with GAPDH K and/or D/E residues, with only one cross-link reported between the two proteins bridging peptides spanning residues 356-384 of AE1.⁷ In this view, it should be noted that results from prior studies suggest that the AE1 N-terminus might not necessarily be the only region of this protein interacting with GAPDH. Finally, (vii) we modeled GAPDH-AE1₁₋₅₆ structural interactions, as constrained by all the data above. We also provide evidence of direct and indirect interactions of the N-terminus of AE1 with several other glycolytic enzymes and show that the metabolic defect in glutathione recycling of oxidatively challenged or stored RBC can be rescued in WT human and genetically ablated mouse RBC through incubation with a

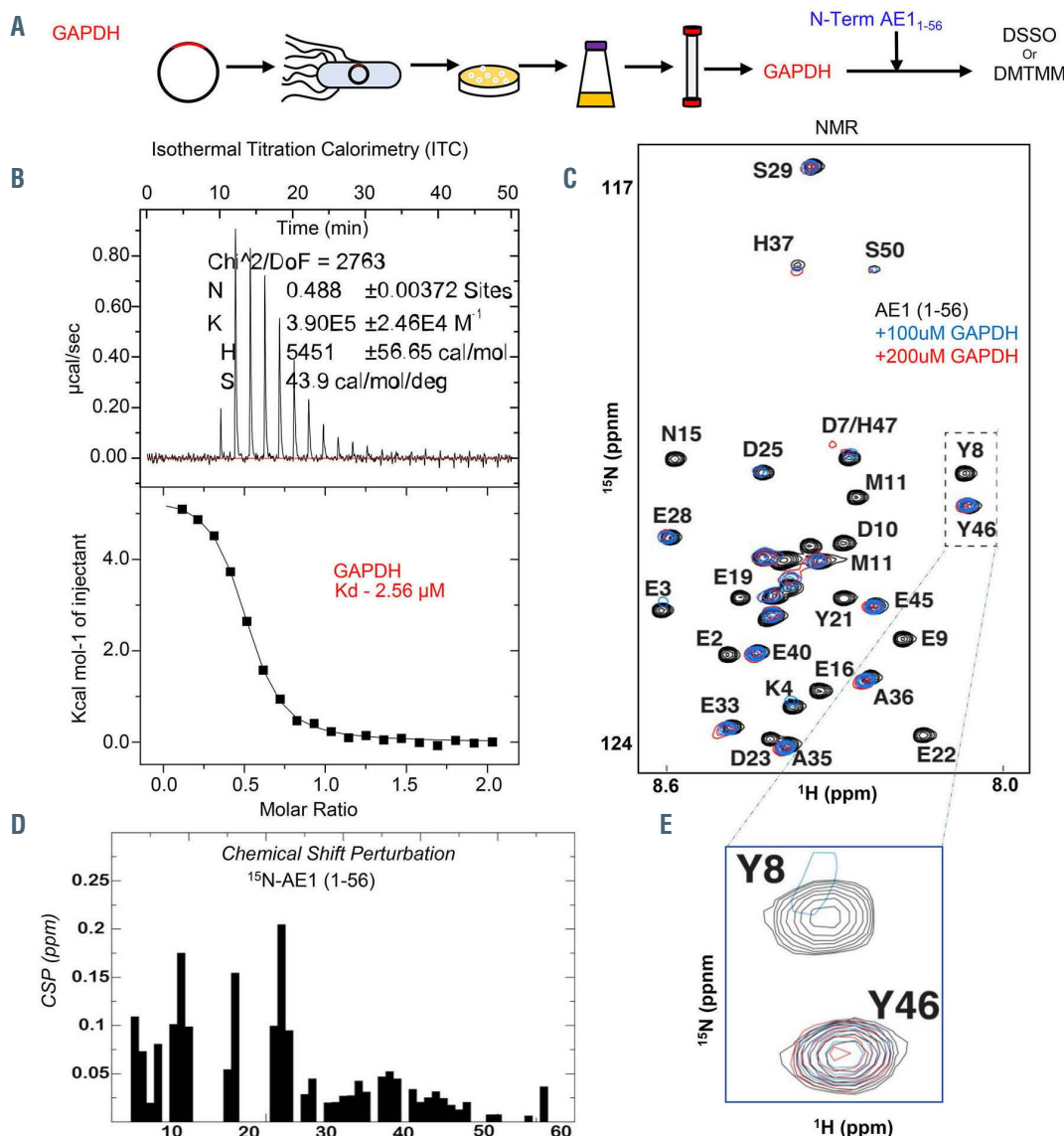


Figure 6. Continued on the following page.

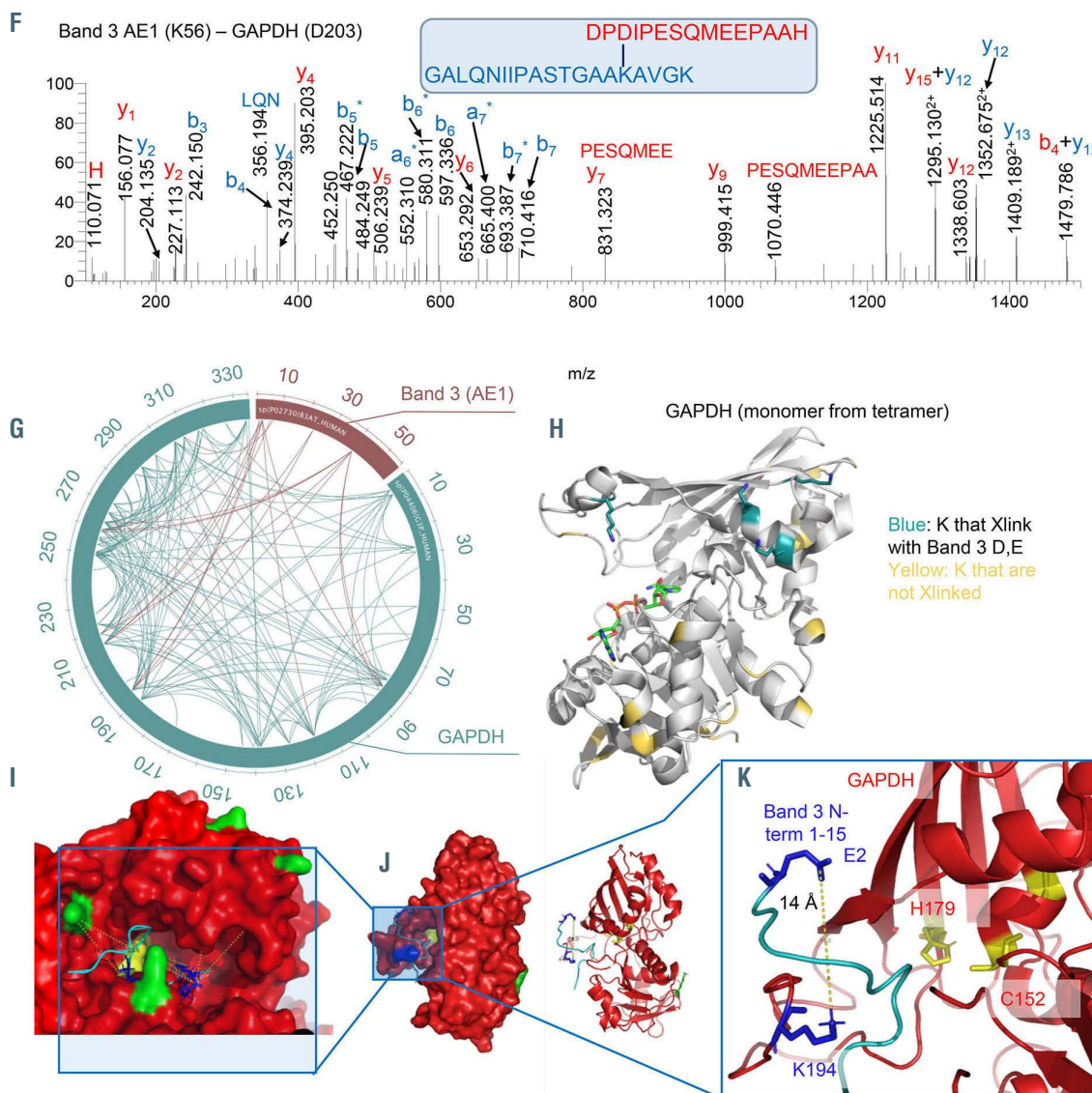


Figure 6. Structural studies of recombinantly expressed GAPDH and its interaction with the N-terminus of band 3 (residues 1-56). (A) Glyceraldehyde 3-phosphate dehydrogenase (GAPDH) was recombinantly expressed in *E.coli* prior to purification and interaction studies with the recombinantly expressed band 3 peptide (residues 1-56). (B-E) These studies included isothermal titration calorimetry (B), nuclear magnetic resonance of band 3 (AE1₁₋₅₆) with 100 or 200 μ M GAPDH (C) and derived calculation of chemical shift perturbations (CSP) (D), and *in silico* modeling of band 3 (1-56) structure based on NMR data (E). Following these studies, crosslinking proteomics analyses were performed *in vitro* by co-incubating GAPDH and AE1₁₋₅₆ in the presence of disuccinimidyl sulfoxide (DSSO) or 4-(4,6-dimethoxy-1,3,5-triazin-2-yl)-4-methylmorpholinium (DMTMM). (F, G) A representative spectrum (F) from one of the most abundant crosslinks, comprehensively mapped in the circos plot (light blue for intramolecular crosslinks, red for intermolecular ones) (G). (H) Results were thus mapped against the GAPDH monomeric structure (blue: all lysine residue on GAPDH that were experimentally found to crosslink to band 3 aspartyl or glutamyl side chains; yellow: the lysines that were available for crosslinking but were not found to face band 3 acidic residues within the reach of the crosslinker of ~20 Å). (H-K) Nuclear magnetic resonance and crosslinking proteomics data were used to build a model of the band 3 (1-56) interaction with GAPDH with the software Rosetta, resulting in the active site pocket of GAPDH being exposed to residues 1-15 of band 3.

cell-penetrating AE1₁₋₅₆ peptide. Clearly, these proof-of-principle mechanistic experiments do not suggest the potential use of such peptides as a supplement to current blood bags, since the approach would be logistically unfeasible because of the prohibitive costs. An additional concern about such an approach would be the potential immunogenicity of such a peptide upon infusion *in vivo*. Notably, activation of the PPP and post-transfusion recovery were normalized in band 3 KO RBC lacking AE1 residues 1-11 (HA Del) upon incubation with a cell-penetrating AE1₁₋₅₆ peptide. It is worth stressing that the band 3 KO mice lacking residues 1-11 (but not those lacking residues 12-23) phenocopied defects in PPP activation previously described in G6PD-deficient RBC^{32,33} with respect to the decreased capacity to activate

the PPP and ultimately poor post-transfusion recovery.

The use of multiple approaches to investigate AE1 interacting partners is justified by the intrinsic limitations of each independent method. For example, false hits may result from nonspecific pull-down in the immunoprecipitation studies or indirect effects of AE1 on the stabilization of multimeric complexes with proteins identified as candidate interacting partners in thermal proteome profiling studies. To mitigate these problems, we performed additional crosslinking proteomics studies, alone or in combination with immunoprecipitation strategies. Acknowledging these caveats, here we validated well-established AE1 interactors (e.g., hemoglobin, ankyrin, spectrin, carbonic anhydrase, glycophorin A), and identified other likely interactors

including several components of glutathione synthesis (e.g., γ -glutamyl cysteine ligase, glutathione synthetase, glutathione recycling (6PGD), glutathione-dependent lipid peroxidation pathways (glutathione peroxidase 4), as well as other antioxidant enzymes (peroxiredoxins 2 and 6, catalase). While peroxiredoxin 2 had been previously suggested to interact with the N-terminus of AE1,⁵¹ here we provide

direct evidence of this interaction. Tracing experiments suggested that RBC lacking the N-terminus of AE1 suffer from an altered degree of *de novo* glutathione synthesis, at least in part explained by altered glutaminolysis and transamination. Indeed, glutamate oxalacacetate transaminase, postulated to be present⁴² but never before identified through proteomics in RBC, was identified as a potential interactor

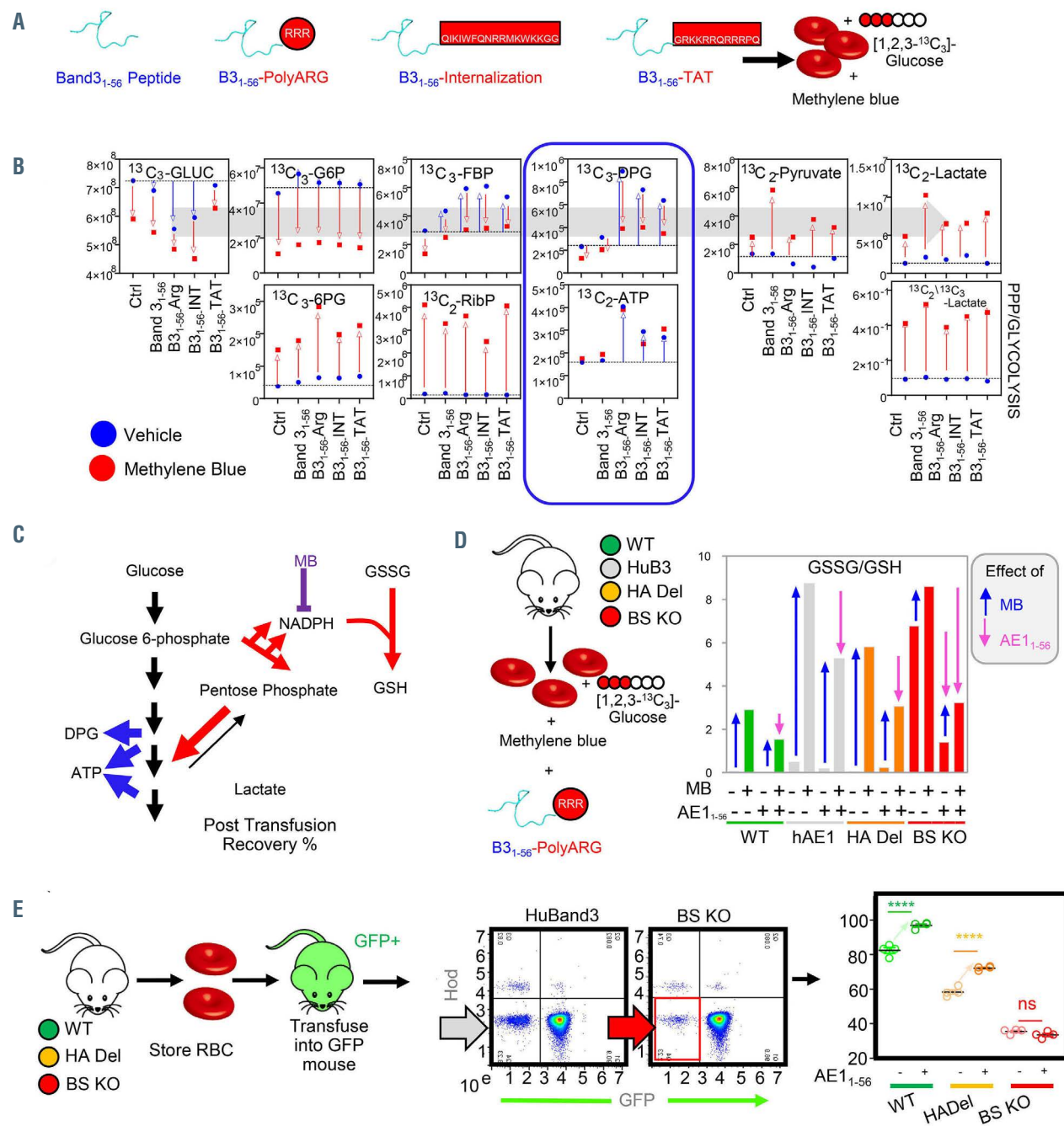


Figure 7. Cell membrane-permeable band 3₁₋₅₆ peptides reverse the defect in the glutathione recycling capacity of red blood cells from band 3 knockout mice. (A) Three membrane permeable versions of the band 3 (AE1₁₋₅₆) peptide were generated through addition of a poly arginine (polyArg), internalization sequence or TAT sequence at the C-terminus of the peptide. Human red blood cells (RBC) were thus incubated with a control (scramble), a band 3 (B3) 1-56 peptide (non-penetrating) or the three penetrating peptides in the presence of 1,2,3-¹³C-glucose and methylene blue (MB) stimulation to activate the pentose phosphate pathway (PPP). (B) ¹³C isotopologues of glycolysis and the PPP are reported for all groups at baseline and following MB stimulation of healthy human RBC, showing increases in PPP activation following MB in all cases, even though ATP levels were only preserved in the RBC treated with the cell-penetrating peptides, suggesting a metabolic reprogramming consistent with the schematic in (C). (D) RBC from wild-type (WT), humanized band 3 (HuB3) or band 3 knockout mice lacking residues 1-11 (HA Del) or 12-23 (BS KO) were stimulated with MB in the presence of a cell-penetrating version of the band 3 peptide (polyArg). Results show increased glutathione oxidation in response to MB treatment in all cases, but significant rescue by the band 3 peptide, especially in the HA Del and BS KO groups. (E) Similarly, storage of murine RBC from the WT and band 3 KO mouse strains in the presence of the polyArg cell-penetrating AE1₁₋₅₆ peptide promoted increases in post-transfusion recovery in WT and HA Del mice, but not in BS KO mice.

with AE1₁₋₅₆. Still, the caveats remain that these interactors would have to compete with a finite number of AE1 N-terminal domains per RBC (~10⁶ copies/cell).

Of note, in the plasma samples we also immunoprecipitated high mobility group nucleosome binding protein and histone H2A type 2, very basic proteins, likely with affinity for the very acidic N-terminus of AE1. While speculative at this stage, if confirmed, this interaction would suggest a role for RBC hemolysis in mitigating the endogenous danger signaling associated with the release of these damage-associated molecular pattern (DAMP) proteins in response to organ damage or traumatic injury or other DAMP-stimulating events.⁵⁴

In conclusion, here we leveraged mouse models carrying a humanized AE1 N-terminus, either canonical or with genetic ablation of sequences coding for amino acid residues 1-11 or 12-23. RBC from these mice, which recapitulate N-terminus AE1 fragmentation observed in human packed RBC during storage in the blood bank or the genetic defect observed in humans carrying band 3 Neapolis, are characterized by increased markers of the storage lesion and poor post-transfusion recovery. Phenotypes recapitulate those observed in humans carrying G6PD-deficient traits in mice lacking AE1 residues 1-11 (which are required for binding to GAPDH in proximity to its active site) and in band 3 Neapolis human RBC, because of defects in the capacity to activate the PPP – a defect that could be mechanistically rescued by a cell membrane-penetrating AE1₁₋₅₆ peptide in proof-of-principle studies. While humans carrying mutations of AE1 N-terminus are not eligible for blood donation, polymorphisms on the chromosome 17 region coding for AE1 are common and associate with an increased susceptibility to lysis following osmotic insult, especially in subjects with single nucleotide polymorphisms targeting residues that we have identified as hotspots for the AE1 N-term interactome (D38, E40 and K56). Finally, here we provide the first experimental map of the RBC interactome (discussed extensively in the *Online Supplementary File*), with a specific focus on the N-terminus of AE1. Through a combination of proteomics approaches (co-immunoprecipitation, thermal proteome profiling and crosslinking proteomics) we validated previously described interactors (e.g., GAPDH) and identified potential new candidate binding partners for AE1₁₋₅₆. Some of the interactions reported here may also be nonspecific (e.g., those driven by electrostatic interactions with the negatively charged acidic

residue-rich N-terminus of AE1) or affected by environmental conditions (e.g., low vs. high oxygen saturation). Further studies will address whether a membrane-penetrating version of the AE1 N-terminus peptide could rescue oxidant stress-induced lesions to RBC AE1 in the context of those pathologies that have been reported to target the N-terminus of AE1, including COVID-19.¹⁸

Disclosures

ADA and KCH are founders of Omix Technologies Inc. and ADA is a founder of Altis Biosciences LLC. AD and JCZ are consultants for Rubius Therapeutics. ADA is an advisory board member for Hemanext Inc. and FORMA Therapeutics Inc. None of the other authors has any conflicts of interest relevant to this study to disclose.

Contributions

ADA, JCZ, SCR and ADO designed the study. AI, JR and EZE performed structural studies. AI, ZD and KCH performed crosslinking proteomics studies. AH and JCZ performed mouse studies. ADA performed metabolomics analyses. AI, MD and KCH performed proteomics analyses; DR and SP enrolled and characterized the band 3 Neapolis patient investigated in the human studies. GP and MPB directed the REDS-III RBC Omics study and related analysis of genome-wide association studies. AI, JCZ and ADA analyzed data. ADA prepared the figures, wrote the first draft of the manuscript and revised it. All the authors contributed to the finalization of the manuscript.

Acknowledgments

The authors are grateful to Devin P. Champagne for his contribution in the early stages of this study.

Funding

This research was supported by funds from the Boettcher Webb-Waring Investigator Award (to ADA), RM1GM131968 (to ADA) and R01GM113838 (to ADO) from the National Institute of General and Medical Sciences, and R01HL146442 (to ADA), R01HL149714 (to ADA), R01HL148151 (to ADA and JCZ), R21HL150032 (to ADA), from the National Heart, Lung, and Blood Institute.

Data sharing statement

Source data for all the figures and analyses in this study are included within *Online Supplementary Table S1*, divided by figures and experiments.

References

- Pantaleo A, Ferru E, Pau MC, et al. Band 3 erythrocyte membrane protein acts as redox stress sensor leading to its phosphorylation by p (72) Syk. *Oxid Med Cell Longev*. 2016;2016:6051098.
- Yoshida T, Prudent M, D'Alessandro A. Red blood cell storage lesion: causes and potential clinical consequences. *Blood Transfus*. 2019;17(1):27-52.
- Bosman GJ, Stappers M, Novotny VM. Changes in band 3 structure as determinants of erythrocyte integrity during storage and survival after transfusion. *Blood Transfus*. 2010;8(Suppl 3):s48-52.
- Bryk AH, Wisniewski JR. Quantitative analysis of human red blood cell proteome. *J Proteome Res*. 2017;16(8):2752-2761.
- Chu H, Breite A, Ciraolo P, Franco RS, Low PS. Characterization of the deoxyhemoglobin binding site on human erythrocyte band 3: implications for O₂ regulation of erythrocyte properties. *Blood*. 2008;111(2):932-938.
- Sega MF, Chu H, Christian J, Low PS. Interaction of deoxyhemoglobin with the cytoplasmic domain of murine erythrocyte band 3. *Biochemistry*. 2012;51(15):3264-3272.
- Puchulu-Campanella E, Chu H, Anstee DJ, Galan JA, Tao WA, Low PS. Identification of the components of a glycolytic enzyme metabolon on the human red blood cell membrane. *J Biol Chem*. 2013;288(2):848-858.
- Sun K, Zhang Y, D'Alessandro A, et al. Sphingosine-1-phosphate promotes erythrocyte glycolysis and oxygen release for adaptation to high-altitude hypoxia. *Nat Commun*. 2016;7:12086.
- Lewis IA, Campanella ME, Markley JL, Low PS. Role of band 3 in regulating metabolic flux of red blood cells. *Proc Natl Acad Sci U S A*. 2009;106(44):18515-18520.
- von Ruckmann B, Schubert D. The complex of band 3 protein of the human erythrocyte membrane and glyceraldehyde-3-phosphate dehydrogenase: stoichiometry and competition by aldolase. *Biochim Biophys Acta*. 2002;1559(1):43-55.
- Eisenmesser EZ, Post CB. Insights into tyrosine phosphorylation control of protein-protein association from the NMR structure of a band 3 peptide inhibitor bound to glyceraldehyde-3-phosphate dehydrogenase. *Biochemistry*. 1998;37(3):867-877.
- Chu H, Low PS. Mapping of glycolytic

- enzyme-binding sites on human erythrocyte band 3. *Biochem J.* 2006;400(1):143-151.
13. Castagnola M, Messana I, Sanna MT, Giardina B. Oxygen-linked modulation of erythrocyte metabolism: state of the art. *Blood Transfus.* 2010;8 Suppl 3(Suppl 3):s53-58.
 14. Rogers SC, Said A, Corcuer D, McLaughlin D, Kell P, Doctor A. Hypoxia limits antioxidant capacity in red blood cells by altering glycolytic pathway dominance. *FASEB J.* 2009;23(9):3159-3170.
 15. D'Alessandro A, Hansen KC, Eisenmesser EZ, Zimring JC. Protect, repair, destroy or sacrifice: a role of oxidative stress biology in inter-donor variability of blood storage? *Blood Transfus.* 2019;17(4):281-288.
 16. D'Alessandro A, Nemkov T, Sun K, et al. AltitudeOmics: red blood cell metabolic adaptation to high altitude hypoxia. *J Proteome Res.* 2016;15(10):3883-3895.
 17. Messana I, Orlando M, Cassiano L, et al. Human erythrocyte metabolism is modulated by the O₂-linked transition of hemoglobin. *FEBS Lett.* 1996;390(1):25-28.
 18. Thomas T, Stefanoni D, Dzieciatkowska M, et al. Evidence of structural protein damage and membrane lipid remodeling in red blood cells from COVID-19 patients. *J Proteome Res.* 2020;19(11):4455-4469.
 19. Chapman RG, Schaumburg L. Glycolysis and glycolytic enzyme activity of aging red cells in man. Changes in hexokinase, aldolase, glyceraldehyde-3-phosphate dehydrogenase, pyruvate kinase and glutamic-oxalacetic transaminase. *Br J Haematol.* 1967;18(5):665-678.
 20. Low PS, Waugh SM, Zinke K, Drenckhahn D. The role of hemoglobin denaturation and band 3 clustering in red blood cell aging. *Science.* 1985;227(4686):531-533.
 21. Rinalducci S, Ferru E, Blasi B, Turrini F, Zolla L. Oxidative stress and caspase-mediated fragmentation of cytoplasmic domain of erythrocyte band 3 during blood storage. *Blood Transfus.* 2012;10(Suppl 2):s55-62.
 22. D'Alessandro A, D'Amici GM, Vaglio S, Zolla L. Time-course investigation of SAGM-stored leukocyte-filtered red blood cell concentrates: from metabolism to proteomics. *Haematologica.* 2012;97(1):107-115.
 23. Reisz JA, Nemkov T, Dzieciatkowska M, et al. Methylation of protein aspartates and deamidated asparagines as a function of blood bank storage and oxidative stress in human red blood cells. *Transfusion.* 2018;58(12):2978-2991.
 24. Kriebardis AG, Antonelou MH, Stamoulis KE, Economou-Petersen E, Margaritis LH, Papassideri IS. Progressive oxidation of cytoskeletal proteins and accumulation of denatured hemoglobin in stored red cells. *J Cell Mol Med.* 2007;11(1):148-155.
 25. Prudent M, Delobel J, Hubner A, Benay C, Lion N, Tissot JD. Proteomics of stored red blood cell membrane and storage-induced microvesicles reveals the association of flotillin-2 with band 3 complexes. *Front Physiol.* 2018;9:421.
 26. Messana I, Ferroni L, Misiti F, et al. Blood bank conditions and RBCs: the progressive loss of metabolic modulation. *Transfusion.* 2000;40(3):353-360.
 27. Tzounakas VL, Kriebardis AG, Georgatzakou HT, et al. Glucose 6-phosphate dehydrogenase deficient subjects may be better "stорers" than donors of red blood cells. *Free Radic Biol Med.* 2016;96:152-165.
 28. Roch A, Magon NJ, Maire J, et al. Transition to 37 degrees C reveals importance of NADPH in mitigating oxidative stress in stored RBCs. *JCI Insight.* 2019;4(21):e126376.
 29. Reisz JA, Wither MJ, Dzieciatkowska M, et al. Oxidative modifications of glyceraldehyde 3-phosphate dehydrogenase regulate metabolic reprogramming of stored red blood cells. *Blood.* 2016;128(12):e32-42.
 30. Azouzi S, Romana M, Arashiki N, et al. Band 3 phosphorylation induces irreversible alterations of stored red blood cells. *Am J Hematol.* 2018;93(5):E110-E112.
 31. Perrotta S, Borriello A, Scaloni A, et al. The N-terminal 11 amino acids of human erythrocyte band 3 are critical for aldolase binding and protein phosphorylation: implications for band 3 function. *Blood.* 2005;106(13):4359-4366.
 32. Francis RO, D'Alessandro A, Eisenberger A, et al. Donor glucose-6-phosphate dehydrogenase deficiency decreases blood quality for transfusion. *J Clin Invest.* 2020;130(5):2270-2285.
 33. D'Alessandro A, Fu X, Kanas T, et al. Donor sex, age and ethnicity impact stored red blood cell antioxidant metabolism through mechanisms in part explained by glucose 6-phosphate dehydrogenase levels and activity. *Haematologica.* 2021;106(5):1290-1302.
 34. Karon BS, Hoyer JD, Stubbe JR, Thomas DD. Changes in band 3 oligomeric state precede cell membrane phospholipid loss during blood bank storage of red blood cells. *Transfusion.* 2009;49(7):1435-1442.
 35. Chu H, McKenna MM, Krump NA, et al. Reversible binding of hemoglobin to band 3 constitutes the molecular switch that mediates O₂ regulation of erythrocyte properties. *Blood.* 2016;128(28):2708-2716.
 36. Howie HL, Hay AM, de Wolski K, et al. Differences in Steap3 expression are a mechanism of genetic variation of RBC storage and oxidative damage in mice. *Blood Adv.* 2019;3(15):2272-2285.
 37. Guo Y, Busch MP, Seielstad M, et al. Development and evaluation of a transfusion medicine genome wide genotyping array. *Transfusion.* 2019;59(1):101-111.
 38. Kanas T, Lanteri MC, Page GP, et al. Ethnicity, sex, and age are determinants of red blood cell storage and stress hemolysis: results of the REDS-III RBC-Omics study. *Blood Adv.* 2017;1(15):1132-1141.
 39. de Wolski K, Fu X, Durmont LJ, et al. Metabolic pathways that correlate with post-transfusion circulation of stored murine red blood cells. *Haematologica.* 2016;101(5):578-586.
 40. Nemkov T, Reisz JA, Gehrke S, Hansen KC, D'Alessandro A. High-throughput metabolomics: isocratic and gradient mass spectrometry-based methods. *Methods Mol Biol.* 2019;1978:13-26.
 41. Reisz JA, Zheng C, D'Alessandro A, Nemkov T. Untargeted and semi-targeted lipid analysis of biological samples using mass spectrometry-based metabolomics. *Methods Mol Biol.* 2019;1978:121-135.
 42. D'Alessandro A, Dzieciatkowska M, Nemkov T, Hansen KC. Red blood cell proteomics update: is there more to discover? *Blood Transfus.* 2017;15(2):182-187.
 43. Franken H, Mathieson T, Childs D, et al. Thermal proteome profiling for unbiased identification of direct and indirect drug targets using multiplexed quantitative mass spectrometry. *Nat Protoc.* 2015;10(10):1567-1593.
 44. Miraglia del Giudice E, Vallier A, Maillet P, et al. Novel band 3 variants (bands 3 Foggia, Napoli I and Napoli II) associated with hereditary spherocytosis and band 3 deficiency: status of the D38A polymorphism within the EPB3 locus. *Br J Haematol.* 1997;96(1):70-76.
 45. Ma SY, Liao L, He BJ, Lin FQ. [Application of high resolution melting curve analysis in detection of SLC4A1 gene mutation in patients with hereditary spherocytosis]. Zhongguo Shi Yan Xue Za Zhi. 2018;26(6):1826-1830.
 46. Weinstein R, Martinez R, Hassoun H, Palek J. Does a patient with hereditary spherocytosis qualify for preoperative autologous blood donation? *Transfusion.* 1997;37(11-12):1179-1183.
 47. Lange PF, Huesgen PF, Nguyen K, Overall CM. Annotating N termini for the human proteome project: N termini and Nalpha-acetylation status differentiate stable cleaved protein species from degradation remnants in the human erythrocyte proteome. *J Proteome Res.* 2014;13(4):2028-2044.
 48. D'Alessandro A, Righetti PG, Zolla L. The red blood cell proteome and interactome: an update. *J Proteome Res.* 2010;9(1):144-163.
 49. Li X, Liu S, Jiang J, et al. CryoEM structure of *Saccharomyces cerevisiae* U1 snRNP offers insight into alternative splicing. *Nat Commun.* 2017;8(1):1035.
 50. Beck KA, Nelson WJ. A spectrin membrane skeleton of the Golgi complex. *Biochim Biophys Acta.* 1998;1404(1-2):153-160.
 51. Matte A, Bertoldi M, Mohandas N, et al. Membrane association of peroxiredoxin-2 in red cells is mediated by the N-terminal cytoplasmic domain of band 3. *Free Radic Biol Med.* 2013;55:27-35.
 52. Ruseska I, Zimmer A. Internalization mechanisms of cell-penetrating peptides. *Beilstein J Nanotechnol.* 2020;11:101-123.
 53. Zhang D, Kiyatkin A, Bolin JT, Low PS. Crystallographic structure and functional interpretation of the cytoplasmic domain of erythrocyte membrane band 3. *Blood.* 2000;96(9):2925-2933.
 54. Silk E, Zhao H, Weng H, Ma D. The role of extracellular histone in organ injury. *Cell Death Dis.* 2017;8(5):e2812.